

Good practice guide for the measurement of BTDF

The following document was prepared in the framework of the EMPIR project 18SIB03 (BxDiff), using the experience from the work carried out in WP2: *Traceable BTDF measurements*. This includes the development of primary BTDF facilities at European national metrology institutes as well as an intercomparison involving several laboratories. The guide is intended to give the reader an overview of the basic definitions of BTDF, suitable measurement set-ups and various factors to consider depending on the sample properties. However, the document is not comprehensive, and the reader is encouraged to seek additional information (e.g., in the listed references [1]-[10]).

1. Introduction

The measurement of BTDF (Bi-directional transmittance distribution function) can be regarded as the transmittance analogue of the BRDF (Bi-directional reflection distribution function) and both are developed from general considerations ([1], [2]) on optical scattering by surfaces and solid bulk material. The BTDF measurand, being dependent on the geometrical parameters of the incident and the transmitted radiation and often denoted as $f_t = f_t(\theta_i, \Phi_i, \lambda, \theta_t, \Phi_t)$, is generally defined as the (infinitesimal) quotient of the transmitted radiance and the illuminating irradiance

$$f_t = \frac{dL_t}{dE_i} \quad (1)$$

In Eq. 1 all geometrical variables are suppressed and other influencing factors, like e.g., the state of polarization, is omitted. In the simplest cases Eq. 1 can be transformed to

$$f_t = \frac{d\Phi_t}{\Phi_i \cos\theta_t d\Omega_t} \quad (2)$$

in which the BTDF appears as the power scattered per unit projected solid angle.

Because of the close relationship between BRDF and BTDF determination, the apparatus used are very similar and the most versatile equipment are goniometric set-ups being able to perform measurements in various geometries. In some commercial set-ups, the absolute BTDF value even relies on a BRDF measurement of a known reflection standard by just moving the detector to the illumination half-plane. Therefore, all dependency on experimental parameters as well as uncertainty considerations can be transferred from the ‘reflection’ to the ‘transmission’ world. However, while for BRDF measurements the solid angle is generally well defined, that is not the case for BTDF measurements on samples with finite thickness. Normally, following the definition of BRDF, the distance is taken from the side of the sample facing the detector although one could argue that the “correct” distance should be somewhere inside the sample. Also, how edge effects due to scattering and reflections inside a sample with finite size should be handled is not clear and will depend on the application or purpose of the measurement. Some advice to care for different input-quantities can be taken from [3] to [5].

Irrespective from different approaches applied, the signals generated by the source and by transmission and there corresponding dark signals must be recorded properly. As the transmitted radiation level may be lower by some orders of magnitude, non-linearity effects must be considered in detection. Influence by wavelength precision and applied spectral bandwidth, the precision of the angular setting, and the applied solid angles in illumination and detection [6] are important parameters to be dealt with. In addition, when using coherent sources or monochromators for illumination, the light is rarely perfectly unpolarised, and care must be taken to avoid errors due to polarisation dependent scattering. Depending on the sample (isotropic or not, degree of scattering etc.) and the measurement geometry, the influence of polarisation will vary but at least for

nonnormal incident angles it is generally recommended to perform measurements with two orthogonal incident polarisations and to average the results.

Transmissive diffusers can be found with a great variation in angular dependence, ranging from Lambertian-like to those showing a pronounced dependence on the transmission angle, the latter often used in beam forming and illumination applications. Where the first usually do not impose great experimental requirements on the size of solid angles, the measurement of the latter require correctly chosen detection settings to avoid larger errors.

2. Measurement methods and set-ups

The key to perform angle-resolved measurements such as BRDF and BTDF, is to be able to orient the sample, the source, and the receiver with respect to one another. The most basic set-up has a fixed source, and simple (1-axis) rotation stages for the sample and the detector. Such a set-up typically only measures the scattered light in the incident plane, thus it is called an *in-plane* design. To perform measurements out of the plane of incidence, the simple rotation stages mentioned above need to be replaced with more complex rotation and movement stages for the sample, the detector or the source, or a combination of them. The most straight-forward way is to allow for the sample to be freely moved and rotated in any orientation, which can be achieved using a Eulerian cradle or a robotic arm to hold the sample. Such set-ups are referred to as *out-of-plane* designs. Some examples of recent BRDF and BTDF measurement systems are given in [4], [7] and [8].

Depending on how the sample is illuminated, absolute BTDF (and BRDF) measurement method can be divided in two different categories. For the *under-filled* method, a relatively small spot on the sample is illuminated and the light scattered into a known solid angle Ω is measured. For a detector with a circular aperture of radius r at a distance R from the sample we have

$$\Omega = \frac{\pi r^2}{R^2 + r^2}, \quad (3)$$

and omitting the differentials in Eq. 2 we get the following expression for the BTDF:

$$f_t = \frac{\Phi_t}{\Phi_i} \frac{R^2 + r^2}{\pi r^2 \cos \theta_t} \quad (4)$$

In most practical cases $r \ll R$ and the r^2 in the numerator in Eq.4 can be omitted with negligible effect on the results. The field of view of the detector must be large enough to include the whole illuminated area on the sample and, depending on the sample and application, surrounding parts illuminated by internal scattering and reflections. The set-up shown in Fig. 1 utilises the under-filled method.

The *over-filled* method relies directly on the radiance-irradiance relationship in Eq. 1 by uniformly irradiate the whole sample and then measure the scattered radiance. However, instead of measuring the irradiance directly, the illumination is normally provided by a source with a uniform radiance L_i over a well-defined opening area. Using the same denotations as above and the relation

$$E_i = L_i \Omega, \quad (5)$$

we get the following expression for the BTDF:

$$f_t = \frac{L_t}{L_i} \frac{R^2 + r^2}{\pi r^2 \cos \theta_t} \quad (5)$$

So, instead of determining the total incident and scattered radiant flux as in the under-filled method, the over-filled method relies on measuring the radiances L_i and L_t . Although both methods can be considered equivalent, in practice, the over-filled method is more seldom used mainly due to the inefficient use of the light resulting in low signal levels.

3. Influence of the apparatus function

A BTDF measurement can only be realized with a finite angle resolution, determined by the geometrical settings given. In the example set-up of Fig. 1 laser sources were used for illumination, delivering expanded beams. Therefore, the main influence on solid angles stems from the detection side. Here, the distance R from the sample to the measurement diaphragm, the diameter d_a of this aperture, and the diameter of the detected area d_s on the sample are the important quantities. As the scattered radiation is imaged on the entrance aperture of an integration sphere, the detected area results from the size of this field aperture by multiplication with the image scale. The resulting resolution of the system can be determined by scanning the illuminating beam without sample, if $d_s < d_a$ is provided and thus d_a is dominating the effective resolution. This resolution will broaden the unknown sample-created distribution and leads to a decrease of the observed maximum as well as to an increase in width.

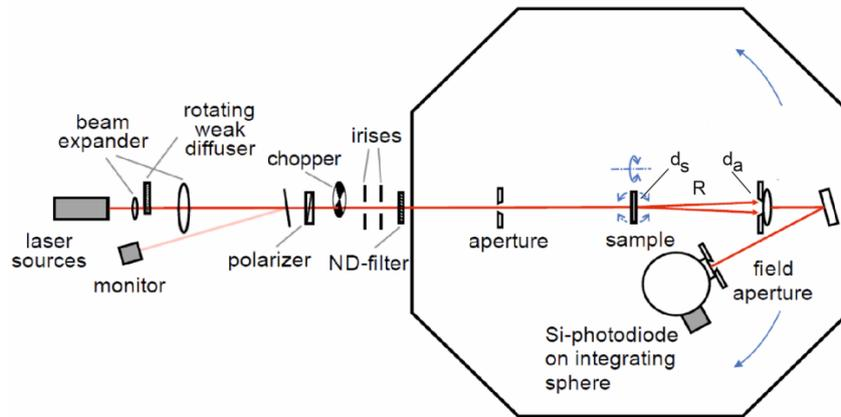


Fig. 1 Example set-up to determine the BTDF of optical diffusers.

From calculation based on gaussian model scatter distributions with full width at half maximum ranging from 10° to 140° , the required resolution of the apparatus can be calculated as a function of a given deviation of the maximum value (geometry $0^\circ, 0^\circ / 0^\circ, 180^\circ$). In Fig. 2 the dependence between the spectrum's FWHM and that of the apparatus function can be read. For a given acceptable deviation, linear functions with varying slope are observed.

E.g., for an accepted deviation of 0.5% the resolution of the apparatus must be $\sim 1/10$ of the scatter distribution width, as shown by the blue line in Fig. 2. To measure with the smallest deviation shown (0.1%), the apparatus function $FWHM_{app}$ must be about a factor 22.5 times smaller than the width of the spectrum.

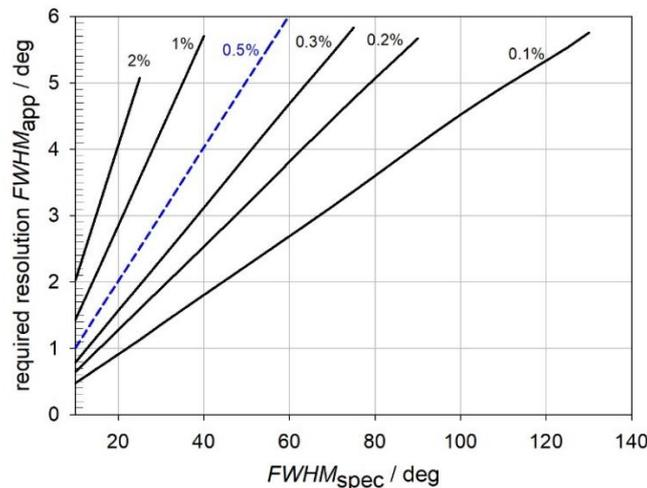


Fig. 2 Required resolution $FWHM_{app}$ of the apparatus needed to obtain a given maximum deviation for spectra with different angular broadness ($FWHM_{spec}$).

Therefore, when characterizing Lambertian-like samples, which often possess widths of larger than 120° and a slowly varying characteristics, an angle resolution of several degrees is sufficient in most cases. For diffusers generating small-width distributions considerably higher resolution is required. E.g., for the distribution of a sandblasted surface shown in Fig. 3, measured with an apparatus function of $\text{FWHM}_{\text{app}} \sim 1.0^\circ$, a deviation for the maximum of $\sim 0.22\%$ is calculated by an unfolding procedure applied on the measured distribution.

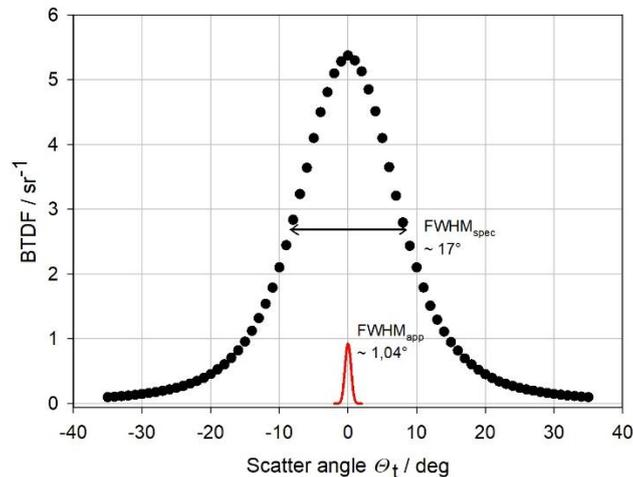


Fig. 3 BTDF scatter distribution for a sandblasted surface diffuser. Red curve: apparatus function.

For the example shown in Fig. 4 measured with a comparable resolution than above, the observed deviation strongly depends on the scatter angle. Whereas the deviation is almost negligible for the flat central part of the distribution, the calculated deviation around and in the nonlinear parts of the steep edges of the rectangular-shaped distribution amounts to about 10-15%.

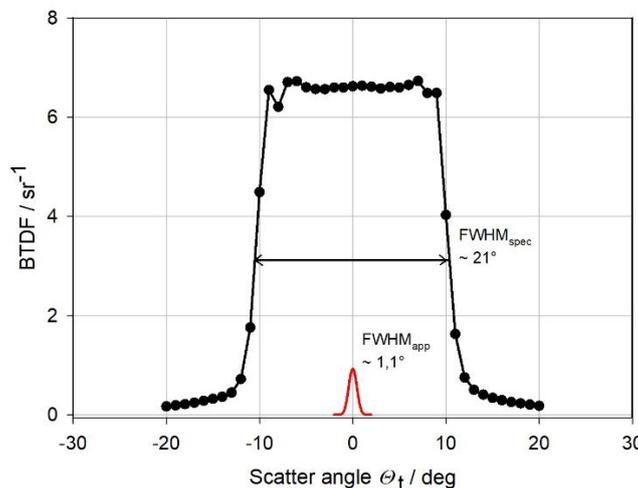


Fig. 4 Rectangular BTDF scatter distribution for an engineered surface diffuser. Red curve: apparatus function.

4. Influence of sample thickness and enhanced lateral scatter

Diffusers showing a high lateral diffusion, either generated by high scattering power or by enlarged thickness of the sample, give rise to experimental problems in so far, as it may become difficult to provide a sufficient large area of detection, especially in the under-illuminated case, where sometimes the illuminating beam cannot be supplied with bigger diameters. In measurements of the sample shown in Fig. 5, which is a Lambertian volume diffuser with a thickness of 2 mm, already some effect can be observed. In the figure the results of measurements are plotted in which the

diameter of the field-aperture of the detection system shown in Fig. 1 and consequently the diameter of the measurement area on the sample was enlarged while keeping the diameter of the illuminated area constant. An increase of the BTDF value can be observed with growing field-stop diameter. Even at the largest available diameter the saturation value is not yet achieved, but the limit value can be taken from the plotted functional dependence. In such a case an overfilled approach, in which the full sample would be homogeneously illuminated by a wide measurement beam would be recommended, or an appropriate correction and uncertainty contribution should be derived from measurements like shown in the figure.

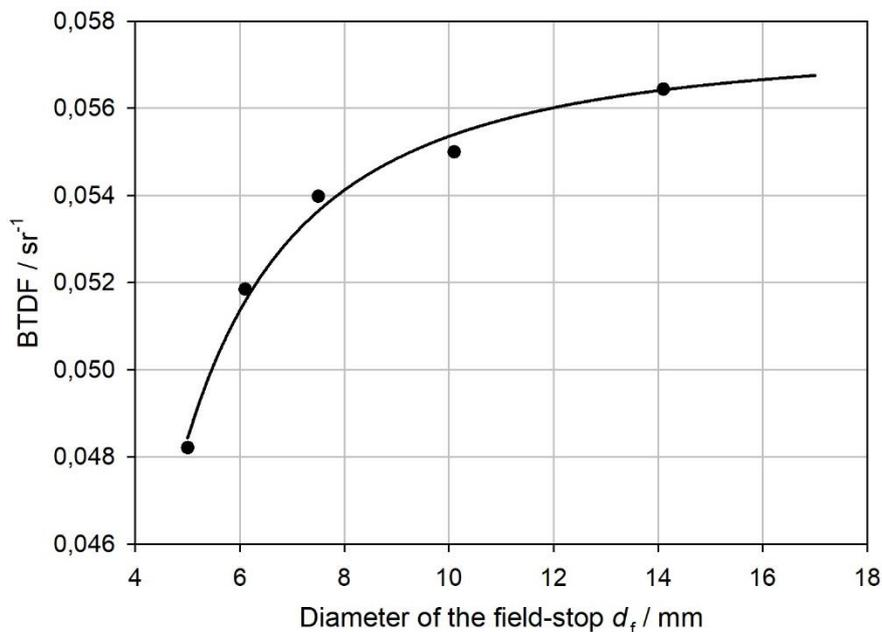


Fig 5 Observed BTDF for a Quartz volume scatterer, measured in straight-on geometry by variation of the field-stop’s diameter at constant illuminated area ($d = 2.5$ mm).

5. Requirements on the field of measurement imposed by structured surfaces

A variety of technical optical diffusers possess structured surfaces and by this intentionally apply some inhomogeneity. These structures are intended to guide incoming radiation into given direction for specific illumination purpose or to homogenize the radiation field and make it less effected by polar incidence and thus better detectable, like e.g., cover glasses of photovoltaic cells. These structures may vary largely in lateral size and can range from micro- to millimetres, imposing requirements on the applied field of measurement. E.g., the scatter distribution shown in Fig. 4 is generated by a small lens-like structures of typically $50 \mu\text{m}$ dimension and the cover plate shown in Fig. 6 has an imprinted surface containing periodic structures with ~ 1.5 mm size.

For comparable measurement results it is required to apply measurement beams with diameters $d_{\text{beam}} > d_{\text{structure}}$, choosing d_{beam} in a way that it averages several ‘periods’ of the structure to minimize spatial inhomogeneity effects. Especially with mm-structures it may be not easy to perform a measurement in an underfilled approach and again an overfilled illumination seems to be preferable in such a case.

Dedicated structures on sample surfaces can also lead to enhanced effects of speckle.

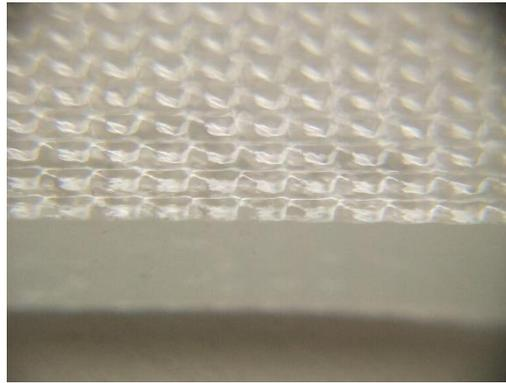


Fig. 6 Microscope image of a cover plate with structured surface produced by imprint technique. Lateral dimension is ~ 1.5 mm.

6. Requirements on the applied radiation field to reduce speckle and interference effects

When reducing spectral bandwidth and / or solid angles in BRDF experiments, speckle structures in the detected reflected radiation fields may occur [9], impeding the extraction of the ‘true’ BRDF value from experiment. The same holds true in BTDF measurements and the effect can be increased by surfaces with dedicated structures, especially when coherent sources like lasers are applied. As an example, the detected radiation behind the sample shown in Fig. 6 is depicted, when measured by a CCD detector. The left image results by just applying the expanded beam of a red HeNe-laser and it shows, besides speckle, even larger interference structures which vary largely in position and intensity if the position of the illumination beam is shifted only slightly across the surface of the sample. The smoother and less position dependent result is shown on the right, achieved when the laser beam first passes a weak rotating diffuser and is then expanded.

More reliable BTDF results are therefore expected if the applied radiation is non-coherent or it is spatially averaged, like e.g., in the example set-up of Fig. 1, in which laser radiation was applied in measurement. When speckle effects cannot be avoided even when taking the described precaution measures, averaging a series of measurements gained with small sample shifts or averaging results for different azimuths may lead to success. The latter, however, is only possible for samples with nominal independence for azimuthal orientation.

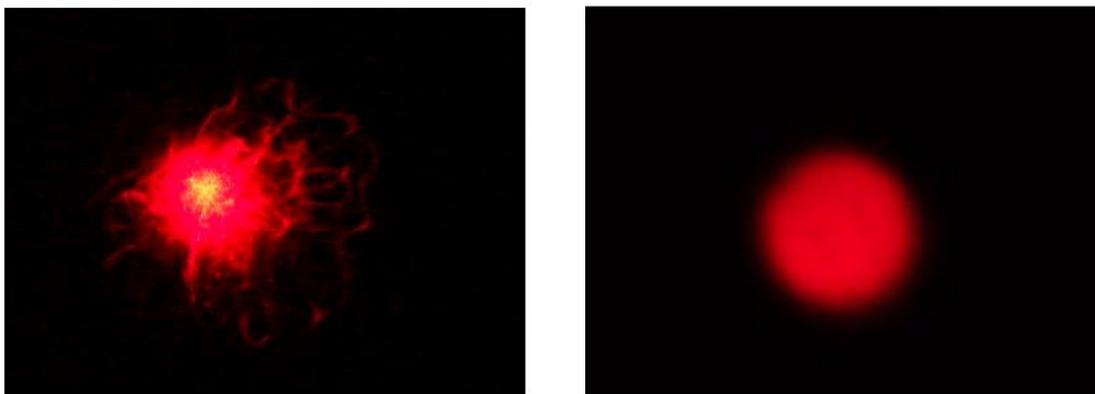


Fig. 7 Transmitted radiation field when the sample shown in Fig. 6 is illuminated by a HeNe laser. Left: coherent expanded laser; right: spatially averaged and expanded.

7. Wavelength dependence

Diffusers used for beam manipulation and illumination purpose are often applied in the complete visual spectrum and a dedicated wavelength dependence is not desired. The usually used material like glass, quartz, polycarbonate, or other clear plastics show only moderate variation. Typically, the in the short-vis wavelength range some absorption will be found and an increase in transmittance for longer wavelengths towards near infrared range.

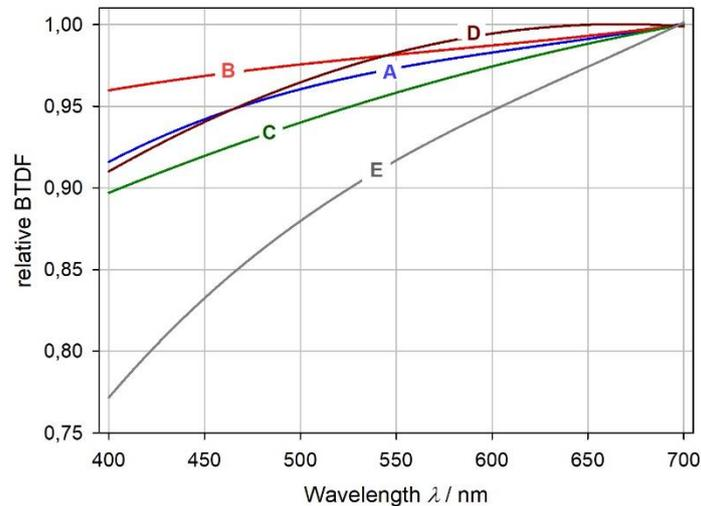


Fig. 8 Wavelength dependence of five optical diffuser types expressed as relative BTDF values for the straight-on scattering situation. A: surface treated polymer; B: fused silica ground glass; C: Quartz with Air-bubbles; D: holographic plastic on glass substrate; E: thin PTFE foil.

In Fig. 8 the relative variation for five diffuser types is shown for the geometry (0° , $0^\circ - 180^\circ$, 0°). The highest variation is found for type E, a small thickness PTFE foil. But even for this type a spectral bandwidth of about 2 nm would not cause noticeable deviation from the true value if applied in measurements.

A subtle effect can be observed for scatter angles other than $\Theta_t = 180^\circ$. In some cases, the wavelength dependence flattens or even changes its sign when Θ_t deviates from the straight-on direction. Then also the width of the scatter distribution changes slightly with wavelength. More information about this effect can be taken from [10].

Acknowledgment

This work was funded by the EMPIR project 18SIB03 (BxDiff). The EMPIR initiative is co-funded by the European Union’s Horizon 2020 research and innovation programme and the EMPIR Participating States.

References

- [1] F.E. Nicodemus, J.C. Richmond, J.J. Hsia, I.W. Ginsberg, T. Limperis, „Geometrical Considerations and Nomenclature for Reflectance“, National Bureau of Standards, Monogr. 160, Gaithersburg, 1977.
- [2] F.E. Nicodemus, „Reflectance nomenclature and directional reflectance and emissivity“, *Applied Optics* 9 (1970) 1474-1475.
- [3] A. M. Rabal, A. Ferrero, J. Campos, J. L. Fontecha, A. Pons, A. M. Rubi no, and A. Corróns, “Automatic goniospectrophotometer for the absolute measurement of the spectral BRDF at in- and out-of-plane and retroreflection geometries,” *Metrologia* **49**(3), 213–223 (2012).
- [4] C. C. Cooksey, J. J. Butler, and G. T. Georgiev, “Comparison of Bidirectional Transmission Distribution Function (BTDF) Measurements on Fused Silica and Sintered Polytetrafluoroethylene Diffusers,” *Metrologia* **56**(6), 065008 (2019).
- [5] I. Santourian, T. Quast, and A. Schirmacher, „Uncertainty budget for PTB’s gonioreflectometers and ways to improve it in the short VIS spectral range“, *Metrologia* **59** (2022) 025004, <https://doi.org/10.1088/1681-7575/ac4e76>
- [6] A. Ferrero, “Theoretical evaluation of the impact of finite intervals in the measurement of the bidirectional reflectance distribution function“, *J Coat Technol Res* **17**, 81–90 (2020).
<https://doi.org/10.1007/s11998-019-00241-2>
- [7][D. Hünerhoff, U. Grusemann, and A. Höpe, “ New robot-based gonioreflectometer for measuring spectral diffuse reflection“, *Metrologia* **43** S11–6, 2006
- [8] A. M. Rabal; A. Ferrero Turrión; J. Campos Acosta; J.L. Fontecha; A. Pons Aglio, M. Rubiño; A. Corróns, „Automatic gonio-spectrophotometer for the absolute measurement of the spectral BRDF at in- and out-of-plane and retroreflection geometries“, *Metrologia*. 49 - 3, pp. 213 - 223. IOP Science, 2012.
- [9] T. Labardens, P. Chavel, Y. Sortais, M. Hébert, L. Simonot, A. Rabal, G. Obein, „Study and simulations of speckle effects on BRDF measurements at very high angular resolution“, *Electronic Imaging*, Volume: 33 | Article ID: art00006, 2021, DOI : [10.2352/ISSN.2470-1173.2021.5.MAAP-140](https://doi.org/10.2352/ISSN.2470-1173.2021.5.MAAP-140)
- [10]) J. Fu, J. R. Frisvad, M. Esslinger, T. Quast, and A. Schirmacher, „Preliminary Results of Angle-Resolved BTDF Characterization of Optical Transmissive Diffusers“, *Colour and Visual Computing Symposium 2022 (CVCS 2022)*, Gjøvik, Norway, September 8-9, 2022, <http://ceur-ws.org/Vol-3271/>, URN: [urn:nbn:de:0074-3271-0](https://nbn-resolving.org/urn:nbn:de:0074-3271-0)